On the evolution of near-singular modes of the Bickley jet

Gordon E. Swaters
Department of Mathematical Sciences and Department of Earth and Atmospheric Sciences, University of Alberta, Edmonton, Alberta T6G 2G1, Canada

(Received 23 September 1998; accepted 23 April 1999)

The linear stability spectrum of the *Bickley* jet has neutral modes which have a phase velocity equal to the maximum jet velocity. Unlike critical levels in monotonic shear flows, the stream function associated with these modes is algebraically singular at the jet maximum. Until recently almost nothing was known about the role these modes played in the stability spectrum of the Bickley jet and that which had been conjectured was, in fact, incorrect. Here, we investigate numerically the nonlinear evolution of ''near-singular'' perturbations in which the phase velocity of the initial perturbation is asymptotically near but not equal to the maximum jet velocity. We show that these modes are surprisingly stable over time. We also show that there is a clearly defined slow time oscillation in the wave number power spectrum of the perturbation stream function which is the result of a slow time oscillation in the underlying modal amplitude. For an initial near-singular mode with a nonzero phase shift across the critical levels, we show that there is a slow time oscillation in the transverse transport of perturbation energy in which the energy flux goes from one critical level to the other and then reverses and so on all the while satisfying no net energy transfer from the mean flow to the perturbation field. © *1999 American Institute of Physics*. [S1070-6631(99)03209-2]

I. INTRODUCTION

Many intense currents of oceanographic and meteorological interest (e.g., western boundary currents and the midlatitude jets) and engineering interest (e.g., the wake behind a bluff body) have flow profiles which have a clearly defined velocity maximum which rapidly fall off to zero in the transverse directions. The stability properties of these flows plays a fundamental role in the transition to turbulence and, for example, the formation of coherent vortex structures in a turbulent fluid.[1,2]

One plane flow profile which has been extensively used to model intense currents is the *Bickley jet*[3,4] where the velocity profile is proportional to $\mathrm{sech}^2(y)$ where y is the transverse coordinate. Originally derived as an approximate steady jet solution to the Prandtl boundary layer equations,[3] the Bickley jet has been used to examine the stability of gaseous jets,[4] midlatitude atmospheric jets,[5] oceanic thermocline jets,[6] and the wake behind a bluff body,[7] among many other applications.

Lipps[5] found both a neutral sinuous and a varicose normal mode solution to the inviscid linear stability problem (i.e., the Rayleigh equation) for the Bickley jet with the critical levels located at the points of inflection given by $y = \pm \tanh^{-1}(1/\sqrt{3})$. Using Lin's perturbation procedure,[8–10] Lipps was able to construct the associated neutral stability boundaries. Howard and Drazin[11] added to the linear stability spectrum by constructing a singular sinuous neutral mode solution to the linear stability problem which had a critical level located at the maximum jet velocity located at $y=0$.

Unlike the perturbation stream function associated with a simple critical level in a homogeneous fluid, the stream function for the Howard and Drazin mode is algebraically singular at the critical level. Howard and Drazin noted that since the location of the critical level does not correspond to an inflection point, this mode was not ''suitable'' for Lin's perturbation formula. Nevertheless, Howard and Drazin concluded that this singular neutral mode did not correspond to a point on a stability boundary. Our understanding of the role that this curious singular mode plays in the stability spectrum of the Bickley jet remained unchanged for the next 27 years.

Maslowe[12] showed, however, based on numerical solutions of the linear stability problem, that the singular neutral mode discovered by Howard and Drazin is indeed part of the lower stability boundary for the varicose mode found by Lipps. Nevertheless, there remain several issues to be resolved concerning this mode. Even though the algebraically singular structure in the stream function of this neutral mode at the critical level is like that encountered in stratified shear flows,[13] Maslowe pointed out that the techniques used in stratified shear flows cannot be used to determine the continuation of the perturbation stream function across the critical level because it is located at a local extremum in the jet profile. Moreover, recent attempts[14] to recover the singular mode as an inviscid limit of solutions to the Orr–Sommerfeld equation[15] have not, as yet, been successful. This suggests that nonlinearity may play a significant role in the spatial regularization of the singularity across the critical level.

It is therefore of interest to determine the nonlinear evolution over time of this singular mode. In this paper we shall address a slightly modified but nevertheless closely related problem. The principal purpose of this paper is to describe the evolution of near-singular modes of the Bickley jet based on nonlinear numerical simulations of the two-dimensional Navier Stokes equations.

By near-singular modes we mean modes for which the

phase velocity is asymptotically close to (but less than) the maximum jet velocity. The leading order far field structure in the transverse direction of such a mode is identical to the Howard and Drazin singular mode. In the immediate neighborhood of the jet maximum, however, the Howard and Drazin algebraically singular critical level bifurcates into a pair of symmetrically placed simple critical levels. By using the parameter which measures the absolute difference between the mode phase velocity and the maximum jet velocity, one can construct an initial condition which does not possess algebraic discontinuities in the stream function. We remark that a similar strategy was qualitatively described by Brunet and Warn[16] and Brunet and Haynes[17] in the context of a Rossby wave on a jet on a β-plane, i.e., a differentially rotating fluid.

Thus, while we are not directly attacking the problem of the nonlinear evolution of the pure Howard and Drazin singular mode, we believe that much can be learned from our results. Moreover, from a phenomenological point of view, it is more likely the case that one would observe a packet of near-singular modes rather than the Howard and Drazin mode in isolation in any event.

It is worth remarking that while much is known about the nonlinear development of critical layers in mixing layers, i.e., monotonic flow profiles,[18–25] there is surprisingly much less known about the nonlinear development of critical layers on jets.[16,17,26,27] The simulations described here, while explicitly focussed on the Bickley jet, nevertheless will be very relevant to the general understanding of the nonlinear evolution of neutral disturbances to fluid jets and the nonlinear dynamics of multiple critical layers that implies.

The plan of this paper is as follows. In Sec. II we formulate the problem we are studying. The initial condition is obtained by constructing a leading order uniformly valid solution to the Rayleigh stability equation for a near-singular normal mode perturbation of the Bickley jet. We discuss the transverse momentum transport and energy flux characteristics of the initial condition. In Sec. III we describe our numerical procedures and the simulation itself. The paper is summarized in Sec. IV.

II. PROBLEM FORMULATION

The nondimensional, incompressible two-dimensional Navier–Stokes equations can be written in the form

$$\Delta\psi_t + J(\psi,\Delta\psi) = \frac{1}{R_e}\Delta^2\psi, \tag{1}$$

where the Jacobian is defined by $J(A,B)\equiv A_xB_y - A_yB_x$ where alphabetical subscripts, unless otherwise noted, imply the appropriate partial derivative, and where the stream function $\psi(x,y,t)$ is related to the velocity field, given by $\mathbf{u}(x,y,t)$, via

$$\mathbf{u}=(u,v)=\mathbf{e}_3\times\nabla\psi=(-\psi_y,\psi_x),$$

and $\Delta=\partial_{xx}+\partial_{yy}$. The orientation of the coordinate system is shown in Fig. 1 and t is time. The Reynolds number is denoted as R_e.

The Bickley jet stream function, given by

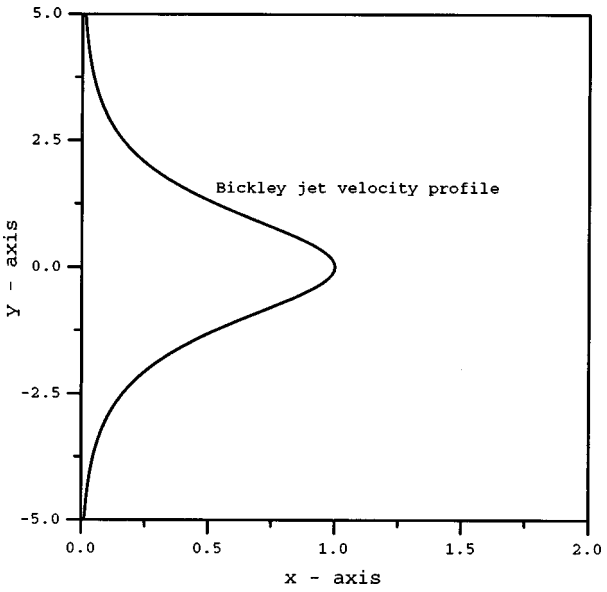

FIG. 1. Geometry of the model used in this paper.

$$\psi=\psi_o(y)=\tanh(y), \quad -\infty<y<\infty, \tag{2}$$

with corresponding velocity field

$$\mathbf{u}=\mathbf{u}_o(y)=(U_o(y),0)=(\mathrm{sech}^2(y),0), \tag{3}$$

is an exact solution to (1) with $R_e=\infty$.

If we assume a perturbed Bickley jet solution to (1) of the form

$$\psi=\psi_o(y)+\{\varphi(y)\exp[ik(x-ct)]+\text{c.c.}\}, \tag{4}$$

where k and c are the real valued x-direction wave number and complex valued phase velocity, respectively, where c.c. means complex conjugate and neglect the quadratic perturbation terms and friction, we obtain the Rayleigh stability equation

$$(U_o-c)(\partial_{yy}-k^2)\varphi - U_{o_{yy}}\varphi=0, \tag{5}$$

which is solved subject to $|\varphi|\to 0$ as $|y|\to\infty$.

The singular neutral mode solution which Howard and Drazin[11] found for (5) is given by

$$\varphi = D\frac{\coth(y)}{\cosh^3(y)} \quad \text{for} \quad (c,k)=(1,\pm 3), \tag{6}$$

where D is a free amplitude constant. We note that this solution is an odd function with respect to y. At the critical level, located at the jet maximum, given by $y=0$, φ is algebraically singular and has the Taylor expansion

$$\varphi \simeq D\left\{\frac{1}{y}-\frac{7y}{6}+\frac{307y^3}{360}-\frac{7717y^5}{15120}+O(y^7)\right\}. \tag{7}$$

Our goal is to describe the evolution of near-singular modes for which

$$k=3 \text{ and } c=1-\varepsilon, \text{ where } 0<\varepsilon\ll 1. \tag{8}$$

We note in passing that while we have chosen to vary the phase velocity in our approach, one could equally well ex-

amine variations in the wave number. Although the examination of that configuration is undoubtedly interesting, we do not pursue it here.

The initial condition for our simulation is constructed from examining the linear asymptotic balances which arise from substituting (8) into the Rayleigh equation (5). We have

$$\left[\frac{1}{\cosh^2(y)}-1+\varepsilon\right](\partial_{yy}-9)\varphi + \left[\frac{2}{\cosh^4(y)}-\frac{4\tanh^2(y)}{\cosh^2(y)}\right]\varphi=0. \tag{9}$$

Assuming we may construct a straightforward asymptotic solution to (9) of the form

$$\varphi\simeq\varphi^{(0)}+\varepsilon\varphi^{(1)}+\cdots,$$

leads to the leading order problem given by

$$\left[\frac{1}{\cosh^2(y)}-1\right](\partial_{yy}-9)\varphi^{(0)} + \left[\frac{2}{\cosh^4(y)}-\frac{4\tanh^2(y)}{\cosh^2(y)}\right]\varphi^{(0)}=0, \tag{10}$$

and the solution for $\varphi^{(0)}$ is given by (6).

However, there is clearly a distinguished limit in (9) for $y\simeq O(\sqrt{\varepsilon})$. Introducing the variable χ, defined by $y=\sqrt{\varepsilon}\,\chi$, and $\varphi=\tilde{\varphi}(\chi)$ into (9) leads to

$$\left[(1-\chi^2)+\frac{2\varepsilon}{3}\chi^4\right](\partial_{\chi\chi}-9\varepsilon)\tilde{\varphi}+(2-8\varepsilon\chi^2)\tilde{\varphi}+O(\varepsilon^2)=0. \tag{11}$$

If we assume a straightforward asymptotic solution to (11) of the form

$$\tilde{\varphi}\simeq\tilde{\varphi}^{(0)}+\varepsilon\tilde{\varphi}^{(1)}+\cdots, \tag{12}$$

the $O(1)$ problem is given by

$$(1-\chi^2)\tilde{\varphi}^{(0)}_{\chi\chi}+2\tilde{\varphi}^{(0)}=0, \tag{13}$$

which has the general solution

$$\tilde{\varphi}^{(0)}=B(1-\chi^2)+A\left[\chi+\frac{1}{2}(1-\chi^2)\ln\left|\frac{\chi+1}{\chi-1}\right|\right], \tag{14}$$

where B and A are arbitrary constants.

The solution for $\tilde{\varphi}^{(0)}$ has two branch points located at $\chi=\pm1$, which correspond to the asymptotically displaced critical levels written in terms of the variable χ. The essential issue is to determine the appropriate relations connecting A and B in the regions $|\chi|>1$ and $|\chi|<1$, respectively.[19,28]

We assume that the argument of the logarithmic term in $\tilde{\varphi}^{(0)}$ is determined by its absolute value and determine B accordingly. This is equivalent to introducing the appropriate branch cut for the logarithmic function when viewed as a complex valued function or, equivalently, the requisite phase shift (if any) across the critical levels. We remark that a version of (14) was obtained by Swaters[29] in a earlier study of neutral perturbations to oceanic jets.

We can immediately see that

$$B\equiv0 \quad \text{for} \quad |\chi|>1, \tag{15}$$

since $\tilde{\varphi}^{(0)}$ as $|\chi|\to\infty$ must asymptotically match with $\varphi^{(0)}$ as $y\to0$ and we note that $\varphi^{(0)}$ and the second term in (14) are both odd functions and therefore have a power series written with respect to odd powers of y and χ, respectively, but the first term in (14), which is proportional to $1-\chi^2$, is even and contains only even powers of χ.

The $|\chi|\gg1$ structure of $\tilde{\varphi}^{(0)}$ is therefore given by

$$\tilde{\varphi}^{(0)}\simeq2A\left\{\frac{1}{3\chi}+\frac{1}{15\chi^3}+\frac{1}{35\chi^5}+\frac{1}{63\chi^7}+O(\chi^{-9})\right\}, \tag{16}$$

or, in terms of y,

$$\tilde{\varphi}^{(0)}\simeq2A\sqrt{\varepsilon}\left\{\frac{1}{3y}+\frac{\varepsilon}{15y^3}+\frac{\varepsilon^2}{35y^5}+\frac{\varepsilon^3}{63y^7}+O(\varepsilon^4)\right\}. \tag{17}$$

Comparing (7) and (17) leads to the relation

$$D=\frac{2\sqrt{\varepsilon}}{3}A. \tag{18}$$

If one were interested in deriving partial differential equations for the space-time evolution of A and B, one would have to examine higher order problems in the asymptotic expansion (including the appropriate slow space and time derivatives). However, as is well known,[30–32] the individual solutions become progressively disordered (i.e., increasingly singular) at the critical levels $\chi=\pm1$. The spatial regularization of the stream function across the critical levels can be achieved by examining sublayers centered at $\chi=\pm1$, respectively, in which physics not included in the Rayleigh stability equation (e.g., time dependence, friction or nonlinearity) cannot be neglected.[16,17,19,28]

While the determination of partial differential equations describing the space-time evolution of A and B is a very interesting and challenging problem, and certainly worthy of study, this is not the approach we take here. Our approach will be to choose *initial* values for A and B consistent with monochromatic critical layer theory and numerically investigate the subsequent evolution of the perturbed Bickley jet.

Because the asymptotically displaced critical levels, located at $\chi=\pm1$, are simple, classical linear viscous critical layer theory[33,15,19] would imply that

$$B=\frac{i\pi A}{2} \quad \text{for} \quad |\chi|<1. \tag{19}$$

On the other hand, if nonlinearity dominates in the critical layer, then it is known[28,34,15] that

$$B=0 \quad \text{for} \quad |\chi|<1. \tag{20}$$

Indeed, as shown by Haberman[34] (see also the discussion in Secs. 27 and 52.5 by Drazin and Reid[15]), the value of B is a monotonic function of the dimensionless parameter $\lambda=(\alpha^{\frac{3}{2}}R_e)^{-1}$, where α is the dimensionless amplitude of the normal mode perturbation. In particular, $B\to0$ as $\lambda\to0$ (i.e., nonlinearity dominates) and $B\to i\pi A/2$ as $\lambda\to\infty$ (i.e., linear viscous dynamics dominates).

It is important to appreciate that (19) and (20) cannot be determined by the present analysis. As mentioned above, one needs to examine sub-layers centered at $\chi=\pm1$, respec-

tively, where the additional physics (i.e., time dependence, friction or nonlinearity) enters into the leading order dynamical balance. In these sublayers, the two individual critical layers centered at $\chi=\pm 1$, respectively, appear as separated, noninflectional, simple critical layers and the results of classical theory[15] will apply.

If we assume that, to leading order, the transverse structure of the *initial* perturbation stream function in the region $y\simeq O(\sqrt{\varepsilon})$ is described by (13), this implies that, at least initially, we are assuming that the nonlinear terms in (1) are small. This, in turn, puts a constraint on our choice of the magnitude of the initial amplitude of the perturbation. If one examines the asymptotic balances which arise by assuming $y\simeq O(\sqrt{\varepsilon})$, $(x,t)\simeq O(1)$ [since $(k,c)\simeq O(1)$ for $(c,k)=(1-\varepsilon,\pm 3)$] and $\varphi\simeq O(A)$, it follows, after substituting (4) into (1), that we must choose $A\simeq O(\varepsilon^2)$ in order that the nonlinear terms will be $O(\varepsilon)$ compared to the leading order linear balance which we insist must be given by (13) at least initially. To this end we introduce the amplitude rescaling

$$A=\varepsilon^2\tilde{A}, \tag{21}$$

with $\tilde{A}\simeq O(1)$ for the initial perturbation stream function with the obvious modifications to B and D.

We are now in a position to give a leading order uniformly valid solution to (9) which is required for our initial condition. The uniformly valid solution[35] is simply the sum of (6) and (14) minus the overlap term D/y and can be written in the form

$$\varphi(y)=\varepsilon A\left\{\frac{2\varepsilon^{3/2}}{3}\left[\operatorname{sech}^3(y)\coth(y)-\frac{1}{y}\right]+\frac{\pi i\delta}{2}(\varepsilon-y^2)H(\varepsilon-y^2)+\sqrt{\varepsilon}y+\frac{1}{2}(\varepsilon-y^2)\ln\left|\frac{y+\sqrt{\varepsilon}}{y-\sqrt{\varepsilon}}\right|\right\}, \tag{22}$$

where we have written this expression with respect to y, dropped the tilde on A and introduced the step function $H(*)=0$ if $*<0$ and $H(*)=1$ if $*\geqslant 0$. In addition, we have introduced, for convenience, the parameter δ which multiplies the contribution associated with the first term in (14). By choosing $\delta=0$ one recovers the value of B associated with a nonlinear critical layer and by choosing $\delta=1$ one recovers the value of B associated with a linear viscous critical layer. Here, we will be primarily focussed on describing the evolution associated the $\delta=1$ initial condition. Note that, whereas in the region $y\simeq O(\sqrt{\varepsilon})$ we have $\varphi\simeq O(\varepsilon^2)$, in the far field $|y|\gg\sqrt{\varepsilon}$ we have $\varphi\simeq O(\varepsilon^{5/2})$. In the numerical simulations, we found it convenient to specify a value for $\varepsilon^{5/2}$ and calculate the other parameters accordingly. Finally, we note, of course, that while $\varphi(y)$ is continuous across $y=\pm\sqrt{\varepsilon}$, its first and higher order derivatives are not.

The initial condition for our numerical simulation will therefore be given by

$$\psi(x,y,0)=\tanh(y)+\{\varphi(y)\exp(3ix)+\text{c.c.}\}, \tag{23}$$

where $\varphi(y)$ is given by (22). In Figs. 2(a) and 2(b) we show

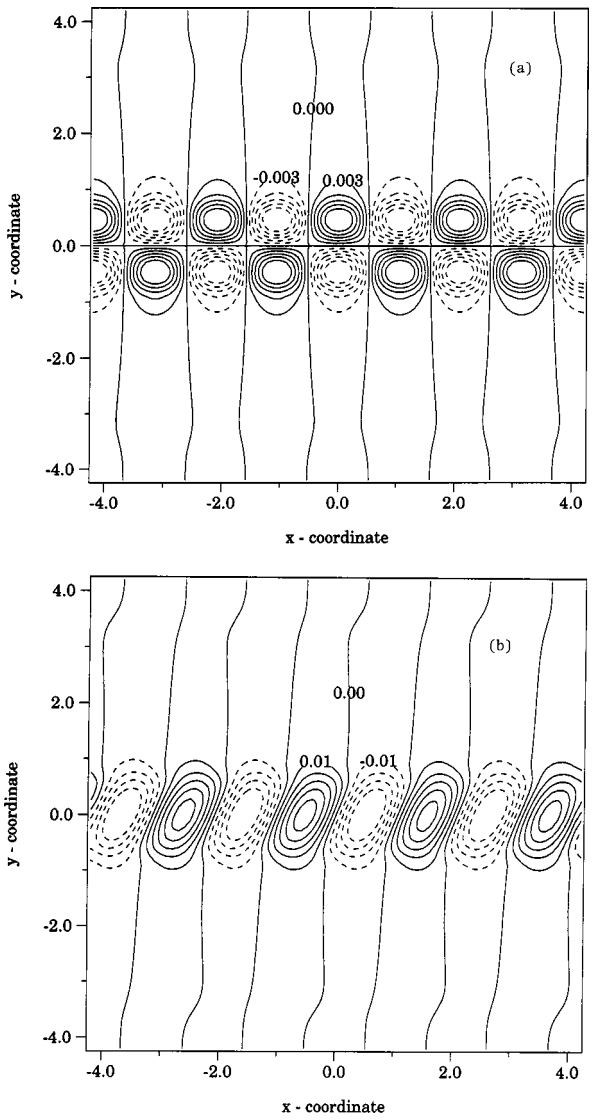

FIG. 2. Contour plots of the initial perturbation stream function for (a) $\delta=0.0$ and (b) $\delta=1.0$, with $\varepsilon=0.3981$ and $A=1.0$. Dashed (solid) contours correspond to negative (non-negative) values of the stream function. The contour intervals are (a) ± 0.003 and (b) ± 0.01.

contour plots of the initial perturbation stream function for $\delta=0.0$ and 1.0, respectively, with $\varepsilon^{5/2}=0.1$ (i.e., $\varepsilon\simeq 0.3981$) and $A=1.0$. The solid (dashed) contours correspond to positive (negative) values of the stream function and the contour interval is ± 0.01.

The presence of the phase shift term proportional to i in (22) has implications for the Reynolds stress and the transverse perturbation energy flux at least initially. The nondimensional Reynolds stress, denoted by τ, averaged over one wave length, is given by

$$\tau=-\frac{k}{2\pi}\int_0^{2\pi/k}u(x,y,t)v(x,y,t)dx, \tag{24}$$

where $u(x,y,t)$ and $v(x,y,t)$ are the real valued x-direction and y-direction perturbation velocities, respectively. Substituting the normal mode representation

$$(u,v)=(-\varphi_y,ik\varphi)\exp[ik(x-ct)]+\text{c.c.}, \tag{25}$$

into (24) leads to

$$\tau = \tfrac{3}{2}\,\mathrm{Im}(\varphi^* \varphi_y), \tag{26}$$

where we have used $(c,k)=(1-\varepsilon,3)$.

We see immediately, of course, that $\tau \equiv 0$ in the regions $|y|>\sqrt{\varepsilon}$ since $\varphi^*\varphi_y$ is real valued because the phase shift term in (22) is not present in these regions. This had to be true since for a neutral mode it is well known[15] that the transverse gradient (i.e., the derivative with respect to y) of the phase averaged Reynolds stress is zero, except possibly at a critical level, and the value of the Reynolds stress at infinity is zero since the entire flow field goes to zero exponentially rapidly as $|y|\to\infty$.

In the region $|y|<\sqrt{\varepsilon}$, however, τ, while of course constant (at least initially), is not necessarily zero. If (22) is substituted into (26), one finds

$$\tau = -\frac{3\varepsilon^{9/2}\pi|\delta A|^2}{2} < 0, \tag{27}$$

in the region $|y|<\sqrt{\varepsilon}$. Thus, for $\delta \neq 0$, the flow associated with the initial perturbation stream function has x-momentum transported in the *negative* y-direction in the $|y|<\sqrt{\varepsilon}$ region.

Associated with the transport of perturbation momentum is an energy transport. The direction of perturbation energy flux in the transverse direction is determined by the sign of[36]

$$\tau(U_o - c). \tag{28}$$

Since $\tau<0$ and $c=1-\varepsilon<U_o$ in the region $|y|<\sqrt{\varepsilon}$, it follows that the initial perturbation field acts to transport perturbation energy in the negative y direction in the $|y|<\sqrt{\varepsilon}$ region. Since $\tau\equiv 0$ in the regions $|y|>\sqrt{\varepsilon}$, there is no energy transport in these regions. The picture emerges in which, averaged over one wave length, the near-singular neutral mode with a nonzero phase shift initially ''extracts'' energy from the Bickley jet at the $y=+\sqrt{\varepsilon}$ critical level and transports it to the $y=-\sqrt{\varepsilon}$ critical level where it is ''redeposited'' back into the mean flow in such a way so that there is no net energy transfer between the Bickley jet to the perturbation field.

One of the principal purposes of this paper is to provide a description of the long time modulation of this process when nonlinearity is present. As our numerical simulations will show, there is a distinct, and previously unreported, slow space-time oscillation in the spectrum and the Reynolds stress of the perturbation field which is directly attributable to this transport.

III. NUMERICAL SIMULATION

Equation (1) was numerically solved as the system

$$q_t + J(\psi,q) = \frac{1}{R_e}\Delta q, \tag{29}$$

$$\Delta\psi = q, \tag{30}$$

where $q(x,y,t)$ is the vorticity. The numerical procedure we use is a second-order accurate 128×128 finite-difference leap-frog technique[37,38] in which the Jacobian term is finite difference using the Arakawa[39] scheme. The Arakawa scheme preserves the skew-symmetry, energy and enstrophy conservation properties of the Jacobian. To suppress the development of the computational mode in the numerical integration a Robert filter[40] is applied at each time step with a coefficient of 0.005. The stream function was obtained at the end of each time step by inverting (30) using a direct solver.

Since the initial perturbation stream function has been chosen on the basis of our examination of the Rayleigh stability equation, we should choose a Reynolds number which is consistent. If one examines the asymptotic balances which arise by assuming $y\simeq O(\sqrt{\varepsilon})$, $(x,t)\simeq O(1)$ and a perturbation stream function amplitude $O(\varepsilon^2)$, it follows, after substituting (4) into (1), that we must choose $R_e \gtrsim O(\varepsilon^{-4})$ in order that, formally at least, $R_e^{-1}\Delta q \lesssim O(\varepsilon)$ compared to the leading order linear balance which we insist must be given by (13) at least initially. In our numerical work, we assume a Reynolds number of $R_e = 3.125\times 10^8$ to effectively smooth out very high wave number features without significantly altering, over the time scales of interest here, the flow evolution. It is our intention to focus on the nonlinear modulation.

Since we are using a leap-frog procedure to numerically integrate forward in time we need initial data not only at $t=0$ but also at the first time step, say $t=\Delta t$. The initial value of the stream function is given by (22) and (23) and the stream function at $t=\Delta t$ is given by

$$\psi(x,y,\Delta t) = \tanh(y) + \{\varphi(y)\exp(3i[x-(1-\varepsilon)\Delta t]) + \text{c.c.}\}, \tag{31}$$

where $\varphi(y)$ is given by (22).

Our simulations are done in a periodic channel domain, denoted as Ω, given by

$$\Omega = \{(x,y) \;|\; |x|<x_L, |y|<y_L\}, \tag{32}$$

in which y_L is chosen so as to have no noticeable effect on the transverse evolution of the perturbation stream function as well as resolving sufficiently the flow in the region $|y|<\sqrt{\varepsilon}$, and x_L is chosen to permit a number of wave lengths. In the simulations described here we choose $x_L = y_L = 4\pi/3$. Thus, for example, if $\varepsilon \simeq 0.3981$ (i.e., $\varepsilon^{5/2}=0.1$), then we will have 12 grid points in the region $|y|<\sqrt{\varepsilon}$.

The value of ε used here will be 0.3981 and we set $A=1.0$. This value for ε can hardly be called asymptotically small. The reason we use it here is purely for expository purposes. The location of the critical levels, given by $\pm\sqrt{0.3981}\simeq\pm 0.6309$, is sufficiently far from $y=0$, that our contour plots of the perturbation fields will be able to clearly show the qualitative structure of the stream function in the interior, i.e., $|y|<\sqrt{\varepsilon}$, and exterior, i.e., $|y|>\sqrt{\varepsilon}$, regions. We computed several simulations with varying values of ε ranging from 0.5 down to 0.05. For the smaller values of ε, it was necessary to introduce a finer 256×256 mesh in order to adequately resolve the transverse structure of the perturbation fields in the interior $|y|<\sqrt{\varepsilon}$ region. In general, we found that we needed at least 10 grid points in the interior

region to have any confidence in the simulation. For values of ε less than about 0.01, it appears that one needs an even finer mesh.

We emphasize that the qualitative features we describe below are representative of all our simulations. Even with $\varepsilon=0.3981$, the actual order of magnitude of the perturbation stream function, compared to the stream function associated with the Bickley jet is, on average, still scale separated so that the dynamics remained weakly nonlinear. Although we did try to run simulations for an initial perturbation corresponding to the ''pure'' algebraically singular Howard and Drazin mode (6), the discontinuity in the stream function at the jet maximum was smoothed out so rapidly by our numerical scheme that we had no confidence in that particular simulation and do not discuss it here. This remains an interesting problem for further investigation. Finally, we remark again, that $\delta=1$ in the initial condition, unless otherwise stated.

We assume that the perturbation stream function, denoted as $\phi(x,y,t)$, i.e.,

$$\phi(x,y,t)\equiv\psi(x,y,t)-\varphi_o(y), \tag{33}$$

satisfies homogeneous Dirichlet boundary conditions on the transverse boundaries, i.e.,

$$\phi(x,\pm y_L,t)=0, \tag{34}$$

and we assume that ψ is smoothly periodic along $x=\pm x_L$. We will denote the initial perturbation stream function $\phi(x,y,0)$ as $\phi_0(x,y)$.

The value of the vorticity on the channel walls was updated using second-order accurate one-sided interior domain differences. We remark that since we are assuming inviscid boundary conditions, this is an appropriate technique for updating the vorticity on the boundaries.

As mentioned above, the we found the near-singular mode to be a remarkably (neutrally) stable perturbation of the Bickley jet for a substantial integration time. In Figs. 3(a) and 3(b) we present contour plots of the perturbation stream function $\phi(x,y,t)$ for $t=87.5$ and 175.0, respectively. The contour intervals in Figs. 3(a) and 3(b) are about ±0.011 and ±0.0099, respectively. The contour labels in each figure (the values -114 and 338 in Fig. 3(a) and -120 and 279 in Fig. 3(b) are 10000 times the actual value of the perturbation stream function.

Comparing Figs. 3(a) and 3(b) with Fig. 2(b) we see that the basic structure of the neutral mode is quite consistent with the initial condition. Of course, the x-direction placement of the highs and lows is different in each frame since the entire field has a phase velocity given by $c=1-\varepsilon\simeq0.6019$. We found that this consistency of the near-singular perturbation stream function held independently of δ and occurred until after $t\simeq250.0$ upon which the jet went unstable. The final instability is the result of numerically introduced perturbations which finally dominate the simulation.

The apparent spatial consistency and surprising stability seen in Fig. 3 suggests that there was very little energy ''leaking'' into other modes in our simulation. To test this assertion we computed the one-dimensional wave-number

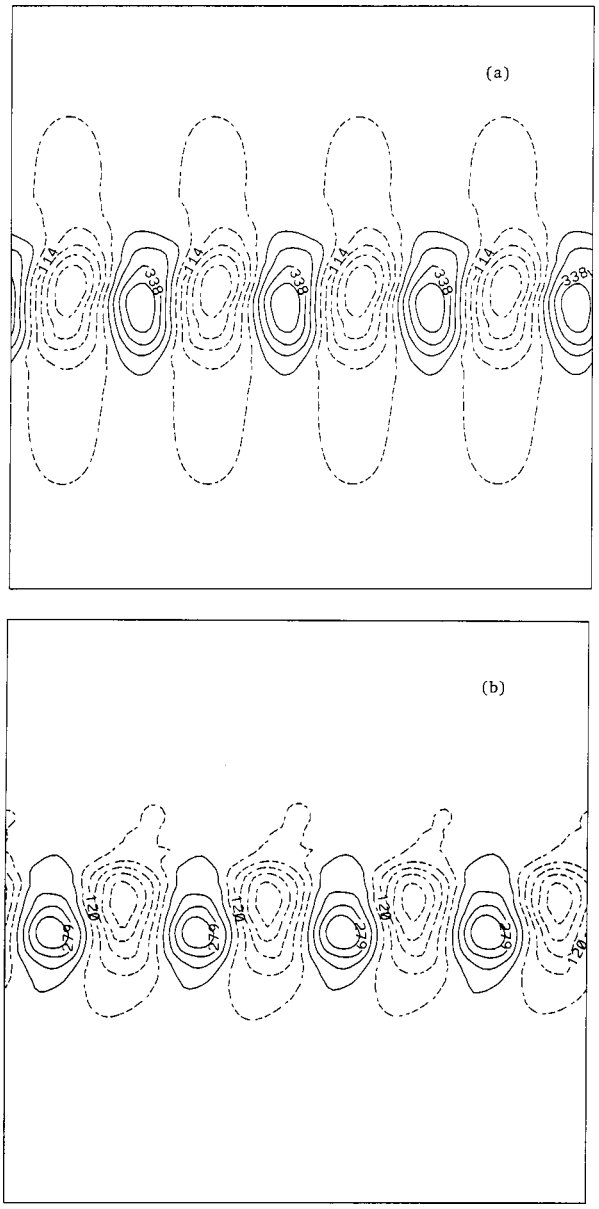

FIG. 3. Contour plots of the perturbation stream function for (a) $t=87.5$ and (b) $t=175.0$, with $\delta=1.0$. Dashed (solid) contours and coordinate axes are as described in Fig. 2. The contour intervals are (a) ±0.011 and (b) ±0.0099.

power spectrum of the perturbation stream function with respect to x. This, by itself, would give a function which depends on the x-direction wave number, given by k, and y and t. Because there was little variation as a function of y, it was convenient to average the resulting spectra over y to come up with a power spectrum for the perturbation stream function which is a function of the x-direction wave number and time alone. We denote the resulting spectrum as $\mathcal{S}(k,t)$ and it is given by (see Jenkins and Watts[41,36] for details)

$$\mathcal{S}(k,t)=\frac{1}{2\pi L^2}\int_{-y_L}^{y_L}dy\left|\int_{-x_L}^{x_L}\phi(x,y,t)\exp(-ikx)dx\right|^2, \tag{35}$$

where $L=2x_L=2y_L$ and where the integrals were evaluated using the trapezoidal rule.

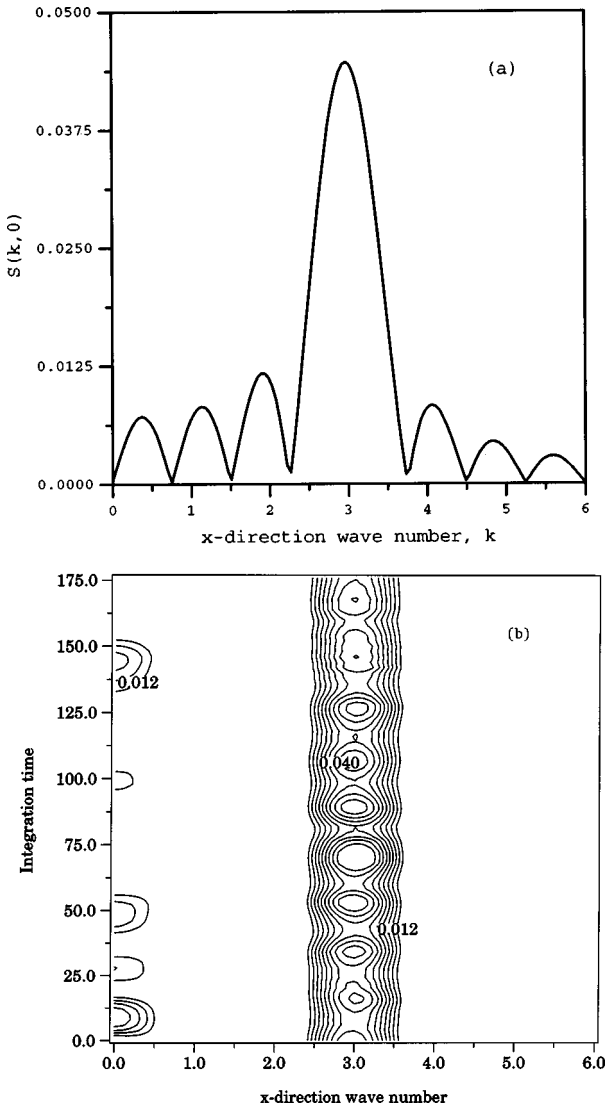

FIG. 4. The y-averaged power spectrum of the perturbation stream function for (a) $t=0.0$ and (b) as a function of wave number and time for $t \in [0,175.0]$. The contour interval in (b) is $+0.012$.

In Fig. 4(a) we show $\mathcal{S}(k,0.0)$. In theory, of course, the spectrum should be a delta function centered at $k=3.0$. We see in Fig. 4(a) a distinct dominant peak at $k=3.0$. The smaller peaks are the result of errors associated with our finite difference representation of the initial data.

In Fig. 4(b) we show a contour plot of $\mathcal{S}(k,t)$ for $t \in [0,175.0]$. The contour interval is 0.012. We see that $k=3.0$ dominates the evolution although there is some energy associated with the low wave number part of the spectrum. Our simulation does not suggest that there is much energy being created at the second harmonic $k=6.0$. We have been unable to determine a satisfactory theoretical explanation for why this should be. (We note that our simulation is able to resolve this wave number since the Nyquist wave number is about 7.6.)

One of the most interesting features seen in Fig. 4(b) is the appearance of an oscillation in time in the magnitude of the peak associated with $k=3.0$. This oscillation occurs over a time scale which is, based on inspection, about 18 time units. This is a time scale which is longer than the period associated with the underlying fast phase oscillation which is given by $2\pi/(ck) \simeq 3.5$ time units. This is suggests the possibility that the underlying amplitude of the near-singular mode may be undergoing ''slow'' time oscillations.

In order to see whether or not the temporal variability seen in $\mathcal{S}(k,t)$ in Fig. 4(b) could be associated with an underlying amplitude oscillation, we computed the area-averaged perturbation kinetic energy normalized by its initial value given by

$$\langle KE \rangle_{\text{pert}}(t) = \frac{\int\int_{\Omega} \nabla\phi \cdot \nabla\phi \, dx\, dy}{\int\int_{\Omega} \nabla\phi_0 \cdot \nabla\phi_0 \, dx\, dy}. \tag{36}$$

Because we are working in a periodic channel, the area integrals in (36) will average out all those spatially periodic contributions for which the domain length is a nonzero integer multiple of the wave length, i.e., the underlying fast phase oscillation. As a result, (36) is a direct measure of the (squared) amplitude of the perturbation field. We observe that the magnitude of the power spectrum $\mathcal{S}(k,t)$ is itself proportional to the (squared) amplitude of the perturbation field. Indeed, due to the strong monochromatic nature of the evolving perturbation stream function, as suggested by Fig. 5(b), we expect that

$$\langle KE \rangle_{\text{pert}} \simeq A^2, \tag{37}$$

where $A(t)$ is the (real valued) time dependent amplitude of the near-singular perturbation stream function with $A(0)=1.0$.

Since we are interested here in not so much as the actual value of $\langle KE \rangle_{\text{pert}}$ as in any possible oscillatory behavior, we calculated the linear trend associated with $\langle KE \rangle_{\text{pert}}$ and computed the residual, i.e., $\langle KE \rangle_{\text{pert}}$ *minus* the trend. The advantage of working with the residual $\langle KE \rangle_{\text{pert}}$ is that when we compute the frequency power spectrum, the ''red'' part of the spectrum will be removed[36] and the variability we are interested in will be highlighted. In Fig. 5(a) we show the residual $\langle KE \rangle_{\text{pert}}$ vs integration time. The underlying periodic behavior is unmistakable. There is a clear oscillatory pattern which occurs at a lower frequency compared to the underlying fast phase oscillation.

In Fig. 5(b) we show the frequency power spectrum associated with the residual $\langle KE \rangle_{\text{pert}}$ as shown in Fig. 5(a). There is a single dominant peak at a frequency of about 0.337 which corresponds to a period about 18.64 time units. For all practical purposes, this is identical to the period seen in Fig. 4(b) for $\mathcal{S}(k,t)$. We therefore attribute the underlying oscillation in $\mathcal{S}(k,t)$ to a ''slow'' time (compared to the fast phase) oscillation in the amplitude of the near-singular perturbation stream function field.

Our numerical experiments suggested that the period of the oscillation seen in Figs. 4(b) and 5(a) is inversely proportional to ε which is expected of course. For $\varepsilon=0.3981$, this is a period on the order of 15.85 time units. Although we have not completed the asymptotic analysis, preliminary analytical results also suggest, that for the near-singular initial condition assumed here, the appropriate ''slow'' time scaling for the nonlinear terms to make an $O(1)$ contribution to the

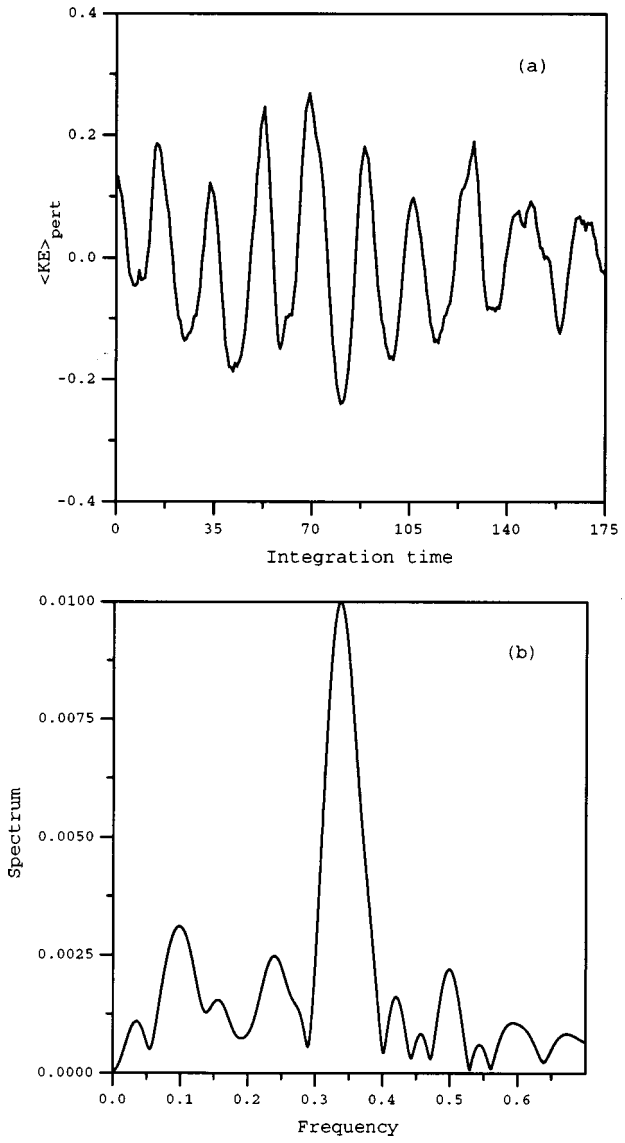

FIG. 5. (a) The area-averaged perturbation energy as a function of time. (b) The frequency power spectrum of Fig. 5(a).

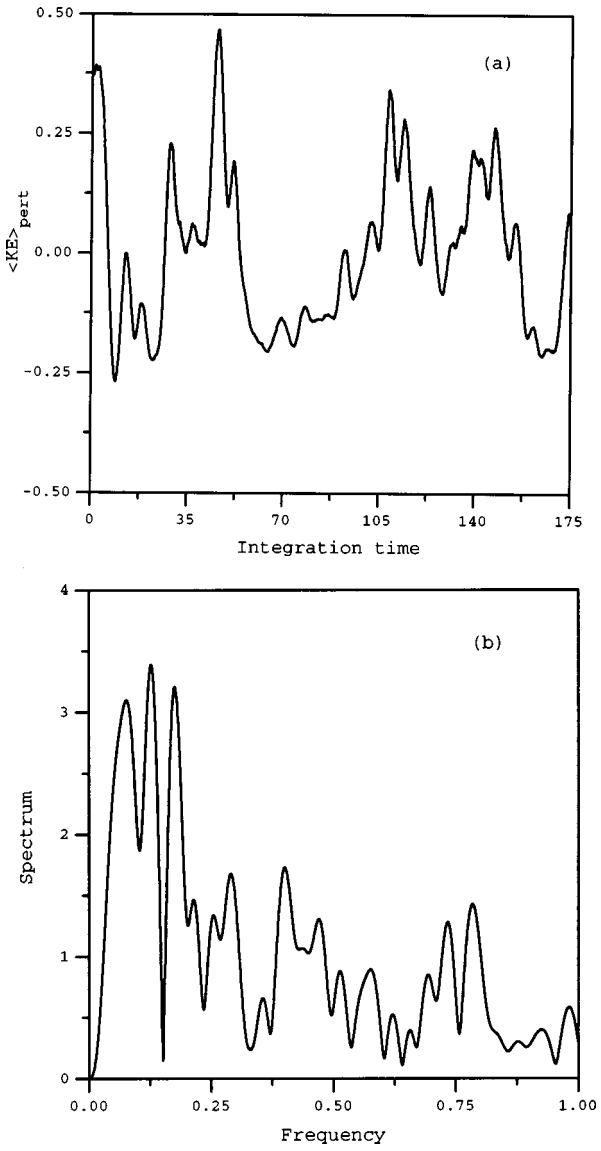

FIG. 6. (a) The area-averaged perturbation energy as a function of time for an initial condition with $\delta=0.0$. (b) The frequency power spectrum of Fig. 6(a).

evolution of the perturbation field is $O(\varepsilon^{-3})$ but this is, as yet, speculative and needs further analysis for confirmation.

We also found that oscillation just described depended on the magnitude of δ in the initial condition. As δ is decreased toward zero we found that regularity of the oscillations diminished and the spectrum became much more broad banded with the spectral peak red shifted. In Fig. 6(a) we show the residual $\langle KE\rangle_{\text{pert}}$ vs integration time for an initial condition with $\delta=0.0$. This value of δ corresponds to the phase shift across the critical layer one would obtain via weakly nonlinear critical layer theory. One sees that while there is still periodic behavior, it much less clearly defined than in Fig. 5(a). In Fig. 6(b) we show the frequency power spectrum associated with Fig. 6(a). One sees that the spectral peak is shifted toward the low frequency part of the spectrum and that there are many other frequencies which make a significant contribution to the evolution. The lack of a clearly defined dominant periodicity can also be seen in $\mathcal{S}(k,t)$ for the $\delta=0.0$ initial condition (not shown here).

When $\delta\neq 0$, there is a phase shift in the initial perturbation stream function across the critical levels which results, as per (27), in a nonzero Reynolds stress and consequently in a nonzero transverse perturbation energy flux. It is obviously of interest to ask how does the Reynolds stress evolve over time in the numerical simulation. As a numerical surrogate for the Reynolds stress, averaged over one wavelength, given by (24) we computed the Reynolds stress averaged over the computational x domain, which we call τ_{num}, defined by

$$\tau_{\text{num}}(y,t)=-\frac{1}{L}\int_{-x_L}^{x_L} u(x,y,t)v(x,y,t)dx, \tag{38}$$

where $u(x,y,t)$ and $v(x,y,t)$ were obtained using second-order accurate finite differences from the perturbation stream function $\phi(x,y,t)$.

In Fig. 7(a) we show $\tau_{\text{num}}(y,0.0)$ vs y (with $\delta=1.0$). We see that the numerically computed Reynolds stress is zero in the regions $|y|>\sqrt{\varepsilon}\simeq 0.631$ and that it is essentially

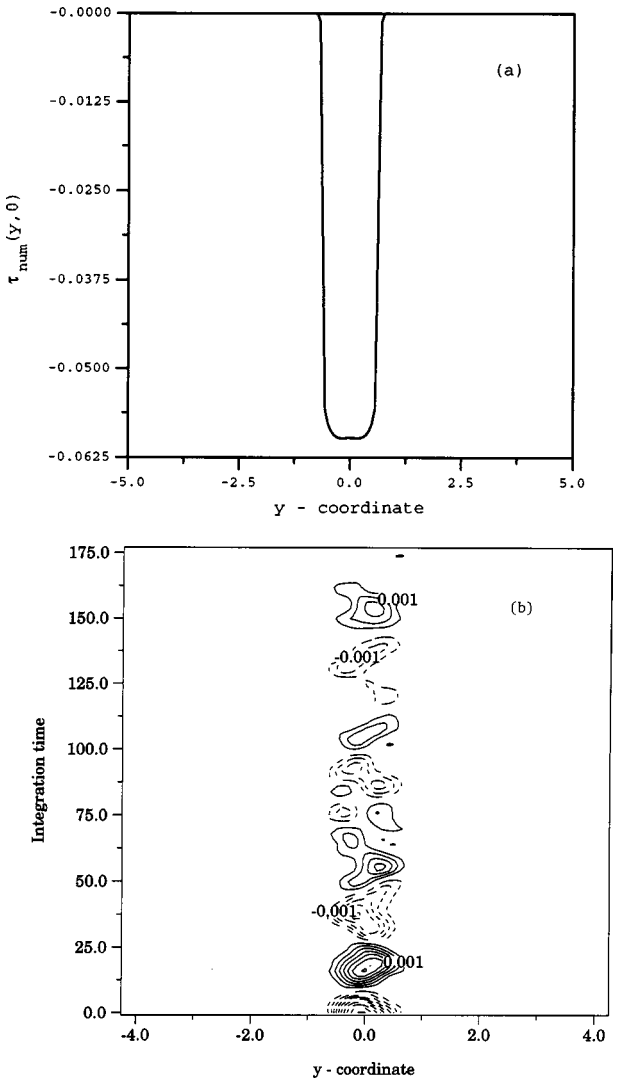

FIG. 7. (a) The Reynolds stress $\tau_{\text{num}}(y,0.0)$. (b) Contour plot of the Reynolds stress $\tau_{\text{num}}(y,t)$ as function of y and time for $t\in[0,175.0]$. The contour interval in (b) is ± 0.001. Dashed (solid) contours are as described in Fig. 2.

constant in the region $|y|<\sqrt{\varepsilon}$ as it must of course. The finite differencing does not do a bad job of representing the transverse structure. We remark that Fig. 7(a) is very similar to the Reynolds stress distribution sketched in Fig. 4.2 by Lin[9] (see also the earlier work by Foote and Lin[42]) for neutral disturbances to a jet. One of our principal objectives is to describe the nonlinear evolution of this Reynolds stress pattern over time.

In Fig. 7(b) we show a contour plot of $\tau_{\text{num}}(y,t)$ over the integration time $t\in[0,175.0]$. The contour interval is ± 0.001. One interesting thing to see in Fig. 7(b) is that the perturbation Reynolds stress is not constant in time. One can see an oscillatory pattern in the Reynolds stress similar to that observed in Figs. 4 and 5. Indeed, since the Reynolds stress is again proportional to the amplitude squared [see Eq. (27)], the peak to trough period is that seen in Figs. 4 and 5. The oscillatory pattern implies that there is an alternating direction to the transverse perturbation energy flux. Initially, in accordance with (28) and the negative sign of $\tau_{\text{num}}(y,t)$, the transverse perturbation energy flux is oriented in the *negative* y direction in the $|y|<\sqrt{\varepsilon}$ region. However, the sign of $\tau_{\text{num}}(y,t)$ subsequently reverses implying that the transverse perturbation energy flux is oriented in the *positive* y direction in the $|y|<\sqrt{\varepsilon}$ region. This pattern continues to oscillate in time.

Another interesting feature in Fig. 7(b) is that there is no perturbation energy flux into the far field over the numerical integration. The Reynolds stress remains zero in the $|y|>\sqrt{\varepsilon}$ regions. Since Fig. 5(a) clearly shows that there is no net energy transfer to the perturbation field (i.e., if instability occurs there would be rapid growth in $\langle KE\rangle_{\text{pert}}$), Fig. 7(b) implies that over time there is an oscillatory pattern being set up in which energy is initially extracted from the Bickley jet at the $y=+\sqrt{\varepsilon}$ critical level and transported, by the near-singular mode, to the $y=-\sqrt{\varepsilon}$ critical level where it is re-deposited back into the Bickley jet. This process reverses itself in time with energy being extracted from the Bickley jet at the $y=-\sqrt{\varepsilon}$ critical level and re-deposited back at the $y=+\sqrt{\varepsilon}$ critical level and so on. This entire cycle occurs without any net energy transfer between the perturbation field and the Bickley jet. This oscillation depends critically on δ. If $\delta=0.0$ initially, there is no initial energy transport and we did not seen any subsequently emerge in the numerical simulation.

IV. SUMMARY

We have investigated numerically the nonlinear evolution of near-singular modes of the Bickley jet. By ''near-singular'' we mean modes for which the phase velocity is slightly less than the maximum jet velocity. Until very recently almost nothing was known about the role that these modes played in the stability spectrum of the Bickley jet since many of the classical techniques of critical layer theory cannot be used to regularize the perturbation stream function across the critical layer if it is centered at the jet maximum.

By using the parameter corresponding to the absolute difference between the modal phase velocity and the maximum jet velocity, we are able to construct a spatially uniformly valid near-singular stream function which can be used as an initial condition in our numerical simulation. In the far field, the initial perturbation stream function appears as a singular mode with the critical level located at the maximum jet velocity. In the near field, near the jet maximum, the critical level bifurcates into two symmetrically placed simple critical levels.

Our simulation has revealed a number of interesting, and previously unreported, features. If the phase shift across the critical levels is initially nonzero so that there is a nonzero Reynolds stress in the region transversely bounded by the critical levels, we have shown that the resulting time evolution is surprisingly monochromatic with a distinct ''slow'' time oscillatory structure in the wave number power spectrum associated with the perturbation stream function. Examination of the de-trended perturbation kinetic energy shows that this oscillation is a consequence of a slow time oscillation in the amplitude in the underlying near-singular normal mode. If one chooses an initial condition with a zero

phase shift across the critical levels, the distinct oscillatory structure in the power spectrum and de-trended perturbation kinetic energy disappears.

We also examined the transverse perturbation energy flux characteristics. For an initial nonzero phase shift across the critical levels, an oscillatory pattern is set up in which energy is extracted from the Bickley jet at one critical level and transported to the other critical level and re-deposited back into the Bickley jet and then back again and so on with no net energy transfer between the Bickley jet and the perturbation field.

It is important to point that in many respects our study is overly idealized. The initial perturbation corresponds to a very special part of the two-dimensional linear stability spectrum of the Bickley jet. We have completely ignored three-dimensional effects or any interactions with other parts of the normal mode spectrum as well as the continuous spectrum. As has been shown by, for example, Criminale *et al.*,[43] the growth of perturbations on jets can be significantly delayed with an appropriate initial condition containing portions of the continuous spectrum. All of these issues need to be fully explored.

ACKNOWLEDGMENTS

The author gratefully acknowledges beneficial discussions with Anthony Davis, Roland Mallier, Sherwin Maslowe, Larry Redekopp, and Tom Warn. Support for the preparation of this paper was provided in part by a Research Grant awarded by the Natural Sciences and Engineering Research Council of Canada and by Science Subventions awarded by the Department of Fisheries and Oceans of Canada and the Atmospheric Environment Service of Canada. Electronic mail: gordon.swaters@ualberta.ca, URL: http://pacific.math.ualberta.ca/gordon/

[1]P. B. Rhines, ''Waves and turbulence on a beta-plane,'' J. Fluid Mech. **69**, 417 (1975).
[2]J. C. McWilliams, ''The emergence of isolated coherent vortices in turbulent flow,'' J. Fluid Mech. **146**, 43 (1984).
[3]W. G. Bickley, ''The plane jet,'' Philos. Mag. **23**, 727 (1937).
[4]P. Savic, ''On acoustically effective vortex motion in gaseous jets,'' Philos. Mag. **32**, 245 (1941).
[5]F. B. Lipps, ''The barotropic stability of the mean winds in the atmosphere,'' J. Fluid Mech. **12**, 397 (1962).
[6]M. Stern, ''The stability of thermocline jets,'' Tellus **13**, 503 (1961).
[7]G. E. Mattingly and W. O. Criminale, ''The stability of an incompressible two-dimensional wake,'' J. Fluid Mech. **51**, 233 (1972).
[8]C. C. Lin, ''On the stability of two-dimensional parallel flows,'' Q. Appl. Math. **3**, 117 (1945).
[9]C. C. Lin, *The Theory of Hydrodynamic Stability* (Cambridge University Press, New York, 1967).
[10]W. Tollmien, ''Ein allgemeines Kriterium der Instabilität laminarer Geschwindigkeitsverteilungen,'' Nachr. Wiss. Fachgruppe, Göttingen, Math-phys. Kl. **1**, 79 (1935). Translated as ''General instability criterion of laminar velocity distributions,'' Tech. Memor. Nat. Adv. Comm. Aero., Wash. **No. 792**, (1936).
[11]L. N. Howard and P. G. Drazin, ''On the instability of parallel shear flow of inviscid fluid in a rotating system with variable Coriolis parameter,'' J. Math. Phys. **43**, 83 (1964).
[12]S. A. Maslowe, ''Barotropic instability of the Bickley jet,'' J. Fluid Mech. **229**, 417 (1991).
[13]P. G. Baines, *Topographic Effects in Stratified Shear Flows* (Cambridge University Press, New York, 1995).
[14]S. A. Maslowe (private communication).
[15]P. G. Drazin and W. H. Reid, *Hydrodynamic Stability* (Cambridge University Press, New York, 1981).
[16]G. Brunet and T. Warn, ''Rossby wave critical layers on a jet,'' J. Atmos. Sci. **47**, 1173 (1990).
[17]G. Brunet and P. H. Haynes, ''The nonlinear evolution of disturbances to a parabolic jet,'' J. Atmos. Sci. **52**, 464 (1995).
[18]K. Stewartson, ''The evolution of the critical layer of a Rossby wave,'' Geophys. Astrophys. Fluid Dyn. **9**, 185 (1978).
[19]T. Warn and H. Warn, ''The evolution of a nonlinear critical layer,'' Stud. Appl. Math. **59**, 37 (1978).
[20]P. Huerre, ''The nonlinear stability of a free shear layer in the viscous critical layer regime,'' Philos. Trans. R. Soc. London, Ser. A **293**, 643 (1980).
[21]P. Huerre and J. F. Scott, ''Effects of critical layer structure on the nonlinear evolution of waves in free shear layers,'' Philos. Trans. R. Soc. London, Ser. A **371**, 509 (1980).
[22]M. E. Goldstein and L. S. Hultgren, ''Nonlinear spatial evolution of an externally excited instability wave in a free shear layer,'' J. Fluid Mech. **197**, 295 (1988).
[23]M. E. Goldstein and S. J. Leib, ''Nonlinear roll-up of externally excited free shear layers,'' J. Fluid Mech. **191**, 481 (1988).
[24]L. S. Hultgren, ''Nonlinear spatial equilibration of an externally excited instability wave in a free shear layer,'' J. Fluid Mech. **236**, 635 (1992).
[25]R. Mallier, ''The nonlinear temporal evolution of a disturbance to a stratified mixing layer,'' J. Fluid Mech. **291**, 287 (1995).
[26]R. Mallier, ''Fully coupled resonant triad interactions in a Bickley jet,'' Eur. J. Mech. B/Fluids **15**, 507 (1996).
[27]S. J. Leib and M. E. Goldstein, ''Nonlinear interaction between the sinuous and varicose instability modes in a plane wake,'' Phys. Fluids A **1**, 513 (1989).
[28]D. J. Benney and R. F. Bergeron, Jr., ''A new class of nonlinear waves in parallel flows,'' Stud. Appl. Math. **48**, 181 (1969).
[29]G. E. Swaters, ''Critical-layer absorption of neutral ageostrophic vorticity wave perturbations of baroclinic jets,'' Geophys. Astrophys. Fluid Dyn. **43**, 1 (1988).
[30]D. J. Benney, ''Nonlinear wave packets on flows with critical layers,'' Stud. Appl. Math. **69**, 177 (1983).
[31]D. J. Benney and S. A. Maslowe, ''The evolution in space and time of nonlinear waves in parallel shear flows,'' Stud. Appl. Math. **54**, 181 (1975).
[32]S. A. Maslowe, ''Evolution equations for finite amplitude wave packets in parallel shear flows,'' Eur. J. Mech. B/Fluids **10**, No. 2-Suppl., 289 (1991).
[33]W. Tollmien, ''Über die Entstehung der Turbulenz,'' Nachr. Ges. Wiss. Göttingen Math.-phys. Kl. 21 (1929). Translated as ''The production of turbulence,'' Tech. Memor. Nat. Adv. Comm. Aero. Wash. **No. 609**, (1931).
[34]R. Haberman, ''Critical layers in parallel flows,'' Stud. Appl. Math. **51**, 139 (1972).
[35]C. M. Bender and S. A. Orszag, *Advanced Mathematical Methods for Scientists and Engineers* (McGraw-Hill, New York, 1978).
[36]P. H. LeBlond and L. A. Mysak, *Waves in the Ocean* (Elsevier, New York, 1978).
[37]J. C. McWilliams, G. R. Flierl, V. D. Larichev, and G. R. Reznik, ''Numerical studies of barotropic modons,'' Dyn. Atmos. Oceans **5**, 219 (1981).
[38]G. E. Swaters, ''A perturbation theory for the solitary drift-vortex solutions of the Hasegawa–Mima equation,'' J. Plasma Phys. **41**, 523 (1989).
[39]A. Arakawa, ''Computational design for long term numerical integration of the equations of fluid motion: Two-dimensional incompressible flow. Part I,'' J. Comput. Phys. **1**, 119 (1966).
[40]R. A. Asselin, ''Frequency filter for time integrations,'' Mon. Weather Rev. **100**, 487 (1972).
[41]G. M. Jenkins and D. G. Watts, *Spectral Analysis and its Applications* (Holden-Day, San Francisco, 1968).
[42]J. R. Foote and C. C. Lin, ''Some recent investigations in the theory of hydrodynamic stability,'' Q. Appl. Math. **8**, 265 (1950).
[43]W. O. Criminale, T. L. Jackson, and D. G. Lasseigne, ''Towards enhancing and delaying disturbances in free shear flows,'' J. Fluid Mech. **294**, 283 (1995).